Derna Academy Journal for Applied Sciences
E-ISSN: 3006-3159
DAJAS

Microstructure Evolution of A356 Alloy Under Modification by Antimony

Abdelfattah. A. Khalil1

Materials Science Department, Faculty of engineering, Omer Al Muktar university, ALBEIDA, LIBYA.

*Corresponding author: E-mail addresses: abdelfatth.ahmed@omu.edu.ly

Volume: 4 **Issue: 1** **Page Number: 15 - 25**

Keywords:
Aluminium alloy A356, Modifier Sb, Optical microscopy, SEM, EDS.

Received: 15\05\2025
Accepted: 30\06\2025
Published: 02\07\2025
DOI: https://doi.org/10.71147/pj9gsv72

ABSTRACT

The effects of antimony (Sb) addition on the microstructure properties of Solidified A356 alloy were investigated. A356–X wt. %Sb (X = 0, 0.1, 0.2 and 0.3) alloys were fabricated using by the permanent mold process. Two different approaches to modification by solidification process have been pursued physically induced and chemically stimulated. The physical relies mainly on the use of external field, such as ultrasonic vibration, while the chemical rout depends primarily on addition of element, which is the subject of this research work. Antimony was used to modify the microstructure of A356 alloy. The effect of addition level of antimony on the solidification of the A356 alloy was investigated and the obtained samples were characterized by optical microscopy, scanning electron microscopy (SEM) and EDS X-ray analysis (EDS). The results showed that: 1)both the dendritic α-Al solid solution and eutectic silicon were significantly modified; 2) the dendritic primary aluminium became globular, and the plate-like or big spherical eutectic silicon turned into fibrous shape and small spheres during the solidification process. The mechanism of the microstructure evolution under inoculated by Sb element was also preliminarily discussed.

1. INTRODUCTION

Water-cooled cylinder blocks, automotive gearbox cases, aircraft fittings and control parts, and other applications requiring excellent castability, good weldability, pressure tightness, and strong corrosion resistance are all made of the common alloy A356 (Zhu M. et, al 2009). Modification of the eutectic silicon from an acicular to a fine fibrous structure can be achieved in two different ways chemical modification (addition of certain elements) and quench modification (rapid cooling rate). Chemical modification is known to occur in a number of elements; the most widely used elements in modern industry are Sr, Na, and Sb. Modification by Sr and Na changes the morphology of eutectic silicon into fine fibrous forms, whereas Sb causes a refinement in the plate like silicon structure.

Additions of other alkali, alkaline earth and rare-earth metals have also been reported to cause modification (Yu-Chou, et. al 2009, Hao Dong, et.al, 2020, Muhammad, et. al 2024**).** It has been found that Sb can effectively refine the Al–Si eutectic structure at casting properties. Sb in the form of Al–Sb master alloys is extensively used as an alternative to Na or Sr in the production of Al–Si alloys by the permanent mold process. In the industrial practice, Sb is often added to the Al–Si melts in the form of Al–Sb master alloy. It has been also reported that Sb results in fine lamellar morphology of eutectic silicon (Karakosea, et.al, 2009, Peng Tang. et. al, 2023). Recently work has indicated that three eutectic nucleation and growth modes are possible in gradient; (Yu-Chou, et. al 2009). Nucleation and growth on the primary aluminium dendrites and , (Hao Dong, et.al, 2020). Independent heterogeneous nucleation of eutectic grains in interdendritic spaces. The authors have recently proposed for causing the observed transition in eutectic nucleation and growth (Kazuhiro. et.al 2001). Modification of aluminum alloys is process by which the melt is deliberately modified by various elements in order to influence the mechanism of eutectic solidification. Modification changes the morphology and size of crystals of silicon (in the case of Silumin), resulting in a notable improvement in mechanical characteristics above those of unaltered alloys. Large silicon crystals reduce the Al-Si alloy's strength characteristics while significantly improving its mechanical qualities as compared to unmodified alloys. The strength of Al-Si alloys is reduced by large silicon crystals. Strength and plastic properties of the modified alloys are therefore higher in comparison to unmodified alloys. Changing the structure may also affect the machinability of the modified alloy. Strength and plastic properties of the modified alloys are therefore higher in comparison to unmodified alloys. Modification is meaningful only for aluminum alloys with a silicon content of more than 5 %(Pavel Kraus1. et.a, 2008).

2. EXPIRMENTS

Materials

The commercial aluminum-silicon based alloy A356 is the material of interest in this study. Table 1 displays its chemical composition, which was supplied by the source "ASTM."

Table 1. Chemical composition of A356 “ASTM”.

Parameter	Values
Min	6.5%Si, 0.20%Mg, Al balance.
Max	7.5%Si, 0.6%Fe, 0.35%Mn, 0.25%Cu, 0.45%Mg 0.35%Zn, 0.25%Ti, other 0.15%, Al balance

Aluminum Company of Egypt supplied this alloy in the ingot form A356, which was subsequently chemically analyzed (real analysis) using the optical immersion procedure. The outcome is displayed in Table 2.

Table 2. Chemical composition of A356.

Values
7.36%Si, 0.15%Fe, 0.00129%Mn, 0.0462%Cu, 0.329%Mg 0.00229%Zn, 0.136%Ti, other 0.012%, Al balance

The aluminium – silicon phase diagram shows that the equilibrium eutectic constitution is about 12.6 wt% silicon. The chosen aluminium alloy in this study consider as in a hypoeutectic Al-Si alloy. Its liquidus temperatures started at 614°C and solidification ended at 577°C (eutectic temperature). The microstructure comprises both primary fcc aluminium solid solution containing 7.36wt% silicon and eutectic containing silicon enriched aluminium and pure silicon (Polmear, 2006).

Addition of of modifier

1500 grams of A356 alloy were melted in a heat resistance furnace with using of a steel crucible coated from inside with graphite. After complete melting of the alloy, the temperature of the molten metal was kept at a temperature of 740 °C± 10 °C, which is higher than its liquidus temperature by about 125 °C to allow the complete dissolution of the silicon particles.

Antimony (Sb) was used in this investigation as a modifier, then treated with addition different amounts of antimony such as 0% , 0.1%, 0.2%, 0.3% respectively. After addition of the modifier, the melt was manually stirred with a steel rod coated with a graphite and was maintained at 740 °C for 5 minutes for homogenization.

Thermocouple type K was used in measuring the temperature during melting process. The thermocouple was calibrated before and after each series of melts.

preparations of Permanent mould

The pouring of melted alloy was carried out into a permanent mould made of cast iron at room temperature. The dimension of permanent mould was 40 mm inside diameter and 200 mm length, as shown in Figure.1

Fig.1 Used permanent mould.

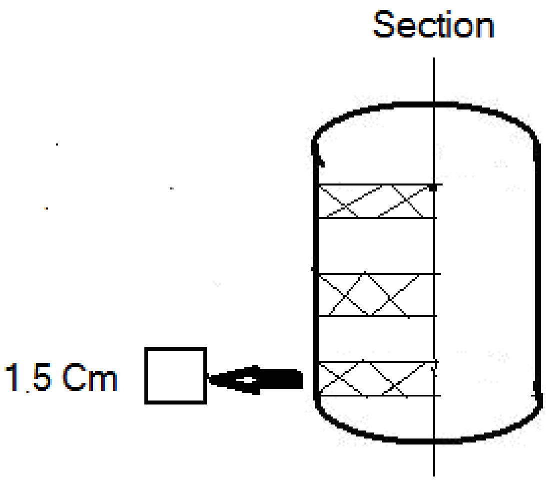

Fig. 2 location of specimens A356

Microstructure Analysis

Metallographic samples were cut from the same position for all experiments 15mm from the bottom of casting as shown in Fig.2 and prepare according to used procedures development for aluminium alloys. Investigated specimens were obtained under addition different amounts of grain refiners such as 0% , 0.1%, 0.2%, 0.3% respectively. Samples for microstructure analysis were taken from each cast sample by sectioning the cylinders parallel to its longitudinal axis, three specimens for microstructure analysis were made from one section, the location of specimens is 15mm respectively from the bottom of cast as shown in Fig.2 Samples were first cut and ground using standard metallographic procedures. They were grinding by using 240, 320, 400, and 600 grit papers. After grinding samples were polished using 1 µm, and 0.05 µm Alumina suspension in water. Final polishing was done using silica suspension. Between each step, samples were thoroughly cleaned.

Optical microscopy and quantitative characterization

Samples used for characterization optical microscopy were etched using 0.5% HF solution to reveal the resulting microstructure (Zhongtao. et.al 2009). Grain size, length, and width of both eutectic silicon and α - aluminium are measured by linear intercept method applied to the microstructure obtained from polarized light in optical microscope at 400X. Six digital micrographs are processed using image C software. Average of ten readings is taken from the results.

Scanning electron microscopic (S.E.M.)

The three-dimensional α-aluminum phase, eutectic Si morphology, and composition of the intermetallic phase presented in the specimens by deep-etched solution were observed using a scanning electron microscope (SEM) equipped with an Energy Dispersive X-ray spectroscopy (EDS) analysis system. In this study, two deep etching techniques were employed. First techniques, specimens were immersed in solution of 30% NaOH in distilled water at temperature of 70 °C for time from 3-20 minutes (ASM, 2005).

The second, specimens were immersed in a solution of 15cm3HCL, 10cm3HF and 90cm3 H_2O (distilled water) for time from 15-20 minutes, then the specimens were immersed in water from 1-2 minutes, then in alcohol for 3-5 minutes, finally the specimens were held in dryer at temperature of 80 °C for 60 minutes (Waly, 1993).

3. RESULTS

Microstructure of A356

Typical optical microscopy images of the A356 alloy with adding the (0, 0.1, 0.2, 0.3) wt. % Sb element are shown in Fig.3. It is clearly seen that in the absence of modifier, the as-cast A356 alloy consists of primary α-Al dendrites and interdimeric needle/plate-like eutectic silicon distributing randomly as shown in Fig. 3a.

However, after adding the antimony element, the microstructures change from coarse dendrites to a fine microstructure, the eutectic silicon needles decrease in size after addition.

The SEM photograph of the sample at different magnification is shown in Fig. 4(a-f). The α- aluminium fully dendritic and large flakes is exhibited in the base aluminium alloy A356. EDS was carried out in the SEM to investigate the nature and composition of samples was characterized by SEM, as shown in Fig. Fig. 5(a, c) shows the three-dimensional SEM morphology of eutectic silicon, the eutectic silicon phase in the original sample exhibited a typical coarse plate-like form, An EDS analysis in the Fig.4(c,d) shows that the eutectic silicon phases with long needle shape are observed in the aluminium matrix.

The effect of Sb on the microstructure of Aluminium alloy A356

Fig. 6(a, b, c, d) reveals the microstructure of A356 alloy inoculated with 0.1% Sb. It is clear that the eutectic silicon needles decrease in size after addition of 0.1% Sb. The results as shown in table.3

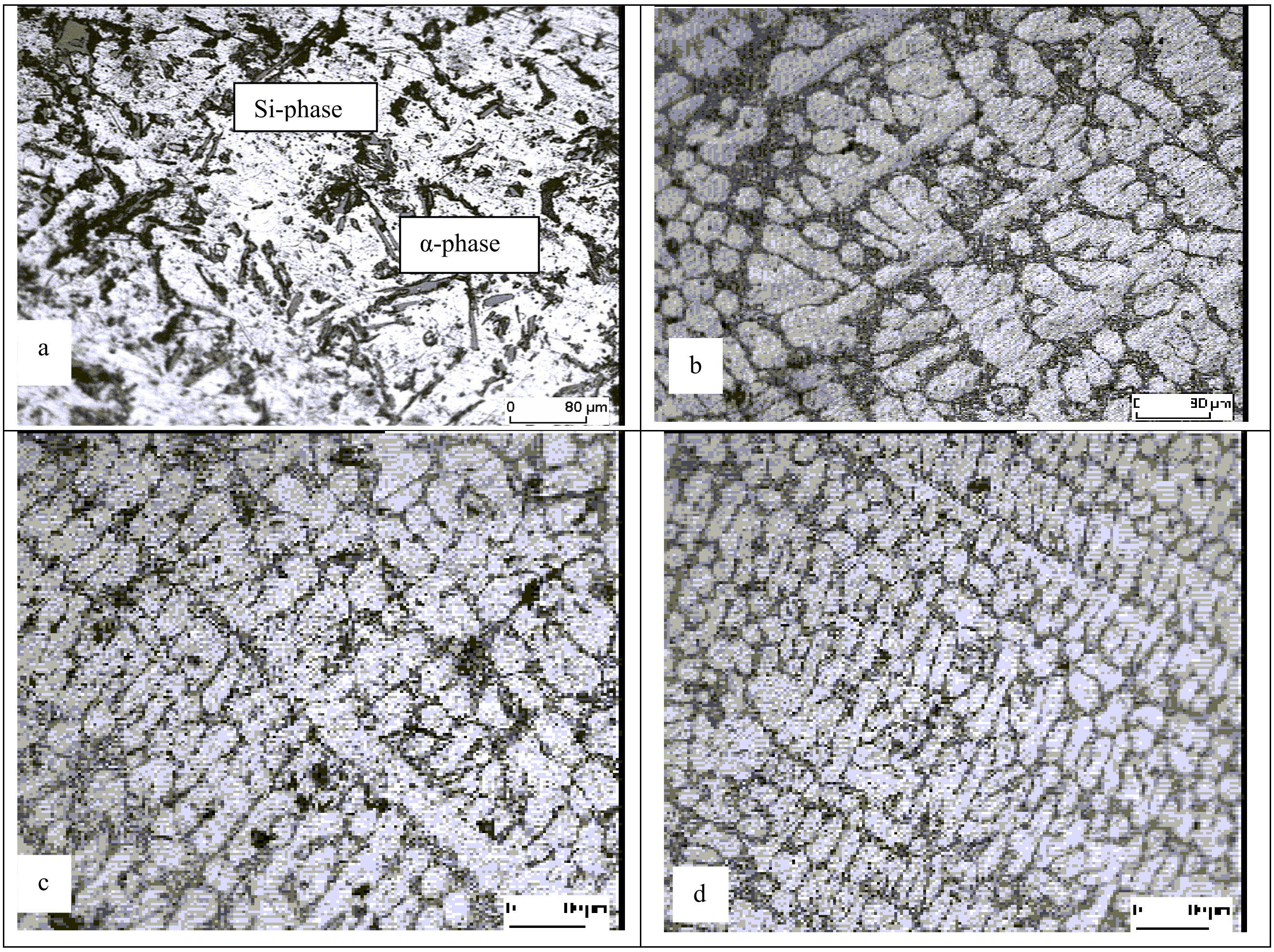

Fig.3 Optical micrograph of A356 modified by a)0 %Sb, b) 0.1 % Sb, c) 0.2 %Sb, d)0.3 Sb.

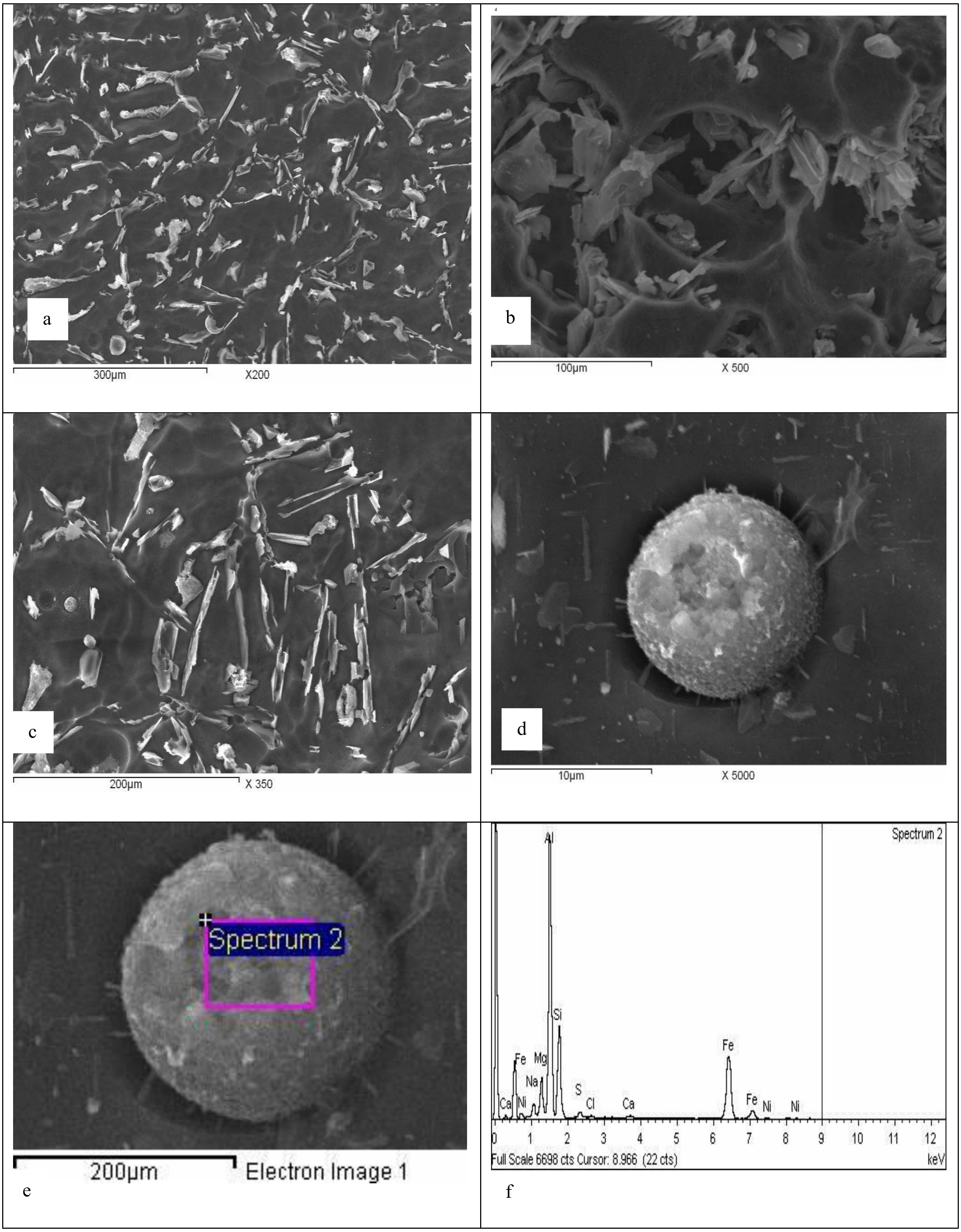

Fig. 4 SEM micrographs a, b, c) and EDS identifications of intermetallics in alloy A356 (morphology of intermetallics (d, e,) (f) composition.

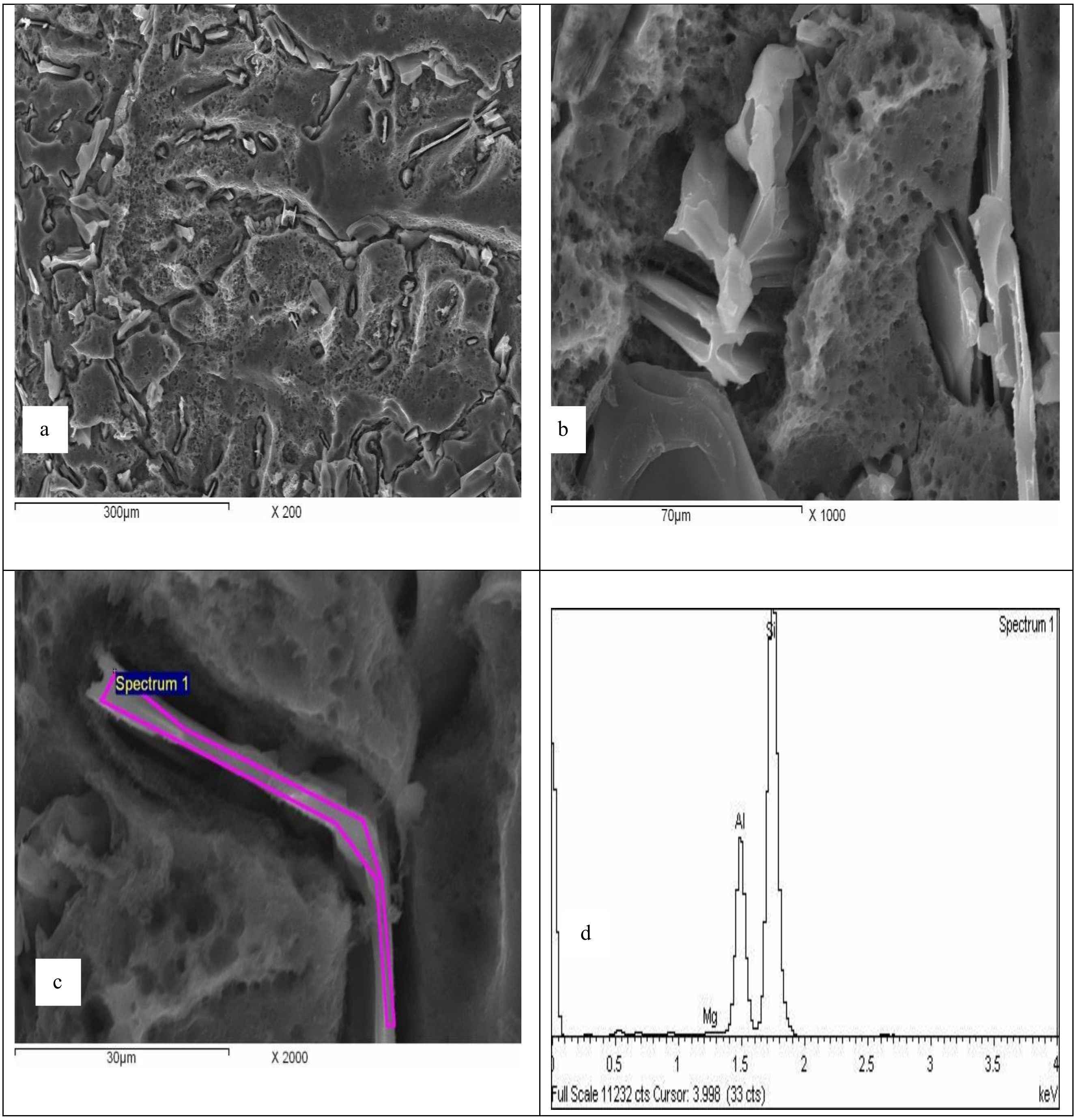

Fig.5 SEM micrographs and EDS identifications of silicon phase in experimental alloy A356 (a&b&c) morphology of silicon phase in base alloy A356; (d) composition analysis of the silicon phase

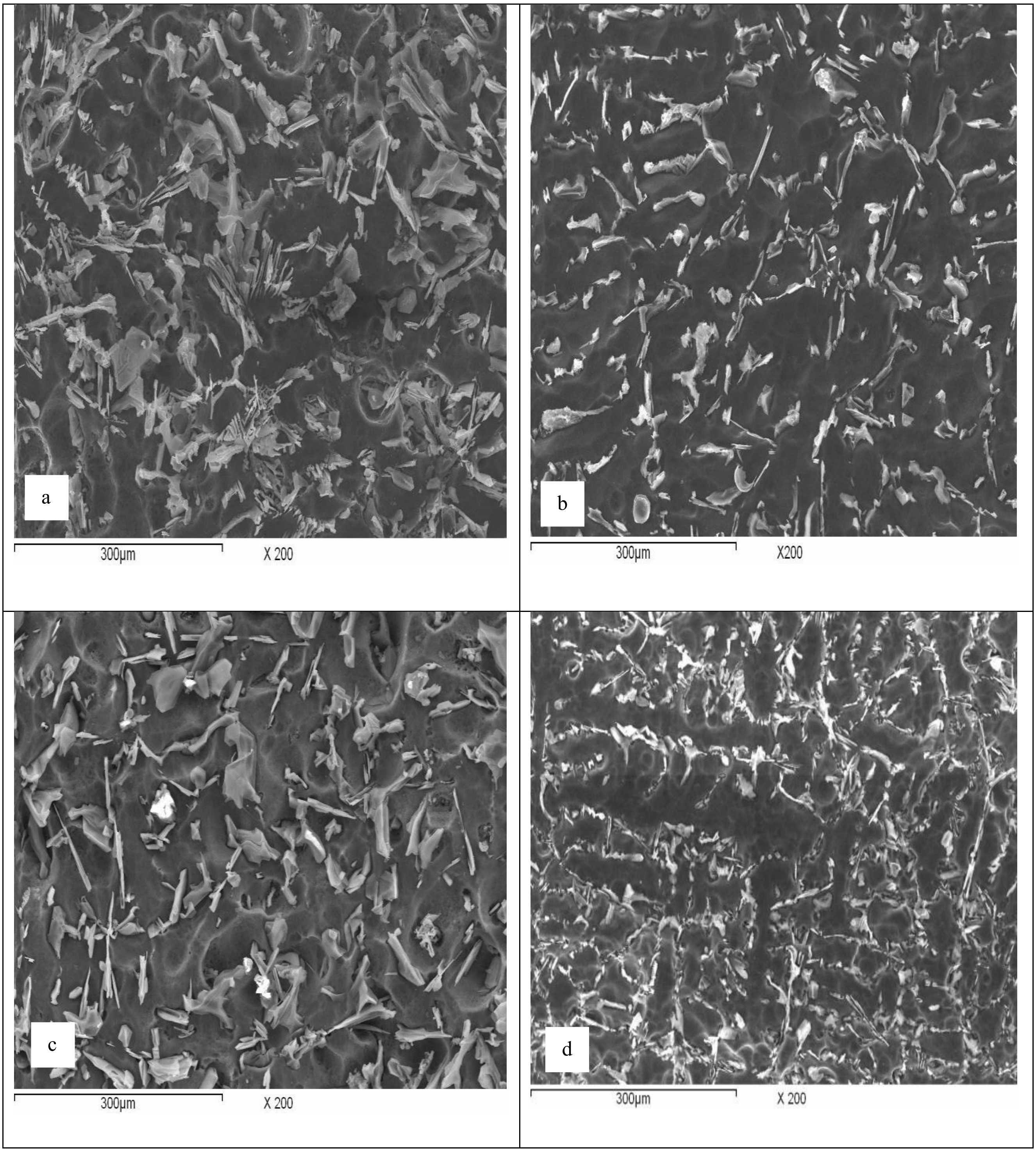

Fig. 6 SEM photomicrographs of the as-cast A356 0 % Sb (a, c), 0.1 Sb % (b, d).

Table 3 Average grain size of α - aluminium

Antimony Wt. %	**0.1%**	**0.2%**	**0.3%**
	320 µm	300 µm	280 µm

4. DISCUSSION

Microstructure of A356

The microstructure of as-cast aluminium alloys A356 was fully dendritic, the original sample exhibited coarse acicular eutectic silicon dispersed among the fully developed primary α-aluminium dendrites as shown in Fig.3(a,), the eutectic silicon was about 32.3 µm in length and average area around 122 μm^2 was also present in the interdendritic areas. One branch of a primary α-aluminium was about 1200 µm in length, as shown in Fig. 3(a), which indicated that the grain size was about a few millimetres as one grain usually contained several arms. The microstructure of hypoeutectic aluminium alloys such as A356, besides a usually coarse and dendritic α-Al solid solution"white" and Al–Si eutectic, where Si usually assumes a long plate or big rounded shape"dark gray". Numerous studies have documented the existence of intermetallic phases that precipitate in the interdendritic and intergranular regions, such as the eutectic Al_2Cu "Chinese script" shaped α- $Al_{15}(Mn,Fe)_3Si_2$ and long, pointed needles of β-$A_{15}FeSi$. (Puga et al , 2011) . The SEM photograph of the sample at different magnification is shown in Fig. 4(a,b). The α- aluminium fully dendritic and large flakes is exhibited in the base aluminium alloy A356. EDS was carried out in the SEM to investigate the nature and composition of samples was characterized by SEM, as shown in Fig. 4(a, b, c, d). It can be clearly seen that the microstructure of the A356 alloy is exhibited fully dendritic for each α- aluminium, silicon phase and other intermetallic phase at a high magnification 350, it can be seen the small sphere particle of intermetallic phase inside the microstructure. An EDS analysis in the Fig4.(e, f) shows that the nature and chemical composition of the small sphere particle shape are observed in the aluminium alloy A356. The EDS X-ray analysis verified that particle shown in the eutectic areas were mainly intermetallic phases and inclusions rather than silicon or aluminium elements. The compound of particle contain the elements Al, Si, Fe and Mg atoms, also other slightly amount of inclusion, element maps also show that the precipitates present (particles within the A356 alloy) are Na, Ni, Ca, S and Cl as shown in element map Fig.4.(f). In the particular case of hypoeutectic A356 alloy, besides a usually coarse and dendritic α- Al solid solution and Al–Si eutectic, where Si usually assumes large plate shape. The chemical composition were detected in non-treated aluminium alloys A356 suggest that they presence of intermetallic phases like the eutectic "Chinese script" shaped α-$Al_{15}(Mn,Fe)_3Si_2$ and long and sharp needles of β-Al_5FeSi, which precipitate in the interdendritic and intergranular regions, while (Puga et al 2011), were reported that The hypoeutectic $AlSi_9Cu_3$ alloy was found to have the same intermetallic phase. In addition to having a very negative impact on the alloy's mechanical characteristics, this morphology. can encourage shrinkage porosity because the platelets physically impede the flow of compensatory feeding liquid, which limits feeding. The distribution of the primary Si phase in the aluminium alloy A356 not treated was not homogeneous, and aggregation was found over the section of the samples Fig. 3(a) and Fig.4 (a). The shapes of the primary Si phase included mostly coarse, large polygon or blocky crystal, The edges and corners of the primary Si phase were clear. The largest length of the primary Si phase was up to 50 µm. Fig. 5(b, c) shows the three-dimensional SEM morphology of eutectic silicon, the eutectic silicon phase in the original sample exhibited a typical coarse plate-like form, An EDS analysis in the Fig.5(c,d) shows that the eutectic silicon phases with long needle shape are observed in the aluminium matrix, The EDS X-ray analysis is shown in Fig. 5(d) verified that those needle shown in the eutectic areas were mainly elemental silicon, rather than intermetallic phases or inclusions. the needle-like compound contain the elements Si, Al and Mg atoms, as showed in Fig. 5(d), but mainly consisted of eutectic silicon phase and aluminium respectively. The formation of needle or long dendritic between primary aluminium phase mainly from silicon has been reported elsewhere (Jiana. et. al, 2006). An aluminum solid solution with slightly more than 1% silicon and nearly pure silicon as the second phase combine to form the eutectic. Although there has been disagreement on the eutectic composition, new experiments using high purity binary alloys have revealed that it is Al–12.6 Si, with the transformation taking place at 577.6 °C. Large silicon plates or needles in a continuous aluminum matrix make up the eutectic, a highly coarse microstructure created by the slow solidification of a pure Al–Si alloy. Fig 4(b). The eutectic itself is composed of individual cells within which the silicon particles appear to be interconnected silicon (Polmear, 2006).

The effect of Sb on the microstructure of Aluminium alloy A356

The as-cast microstructures of A356 alloys with different concentration of Sb (0.1%, 0.2%, 0.3%) respectively. Fig. 3(b, c, d) shows the optical photo micrograph of as cast A356 alloy without addition of Sb. The microstructures seen reveal coarse platelets of eutectic silicon and dendrites of α-Al as shown in Fig. 5(a, b).

Fig. 3 (b) and Fig. 5(c, d) represent the microstructure of A356 alloy inoculated with 0.1% Sb. It is obvious that the eutectic silicon needles decrease in size after addition of 0.1% Sb.

Also, it is evident that the size of eutectic silicon needles becomes finer. Fig.3 (c, d) represents the microstructure of A356 alloy inoculated with 0.2% Sb and 0.3% Sb. It is obvious that the eutectic silicon needles decrease in size after addition of 0.2% Sb. It is evident that the size of eutectic silicon needles becomes more finer at inoculated with 0.2% Sb than at 0.1 % Sb. Fig.3 (b,c) also exhibit the similar behavior as in the case of 0.2 and 0.3% addition level of Sb. However, addition of Sb modifiers to the A356 alloy altered the morphology of the eutectic silicon from coarse acicular to lamellar or fibrous shape, as illustrated in Fig. 3(b, c, d), and Fig.5(c, d) respectively. Most of the silicon particles were transformed to rod shape with blunted tips in Fig.5(c, d) and rounded shape in Fig.5(c). Acicular Si phase was completely absent and coarse type structure turned to fully modified structure.

Also, average grain sizes at different levels of Sb element were calculated using linear intercept method quantitatively analyzed software, the results as shown in table 3. The average grain size of A356 without addition of modification was several millimetres. This result is in accordance with previous work (Jiana. et.al, 2005).

Upon inoculated by Sb element, the dendritic structure was broken up and converted into a somewhat globular grain structure as shown in Fig.3(d).. The average grain size was about 320 μm as shown in table.3

The decrease in grain size could be associated with addition level of Sb element. While increase addition of Sb element from 0.1% to 0.2% led to decrease in grain size from 320 to 300 μm. However, when addition was increased to 0.3 % , the grain size increase to 280 μm, there is significant grain size difference between different level of Sb element alloy was measured. Table. 3 shows the effect of various amounts of Sb modifier on the average grain size of the cast specimens. It can be seen that the increase of Sb element from 0 to 0.1 wt.% in the alloy can result in a fine microstructure and almost significant reduction of the average grain size. However, by further addition of grain refiner (0.2, 0.3 wt.%) to the alloy, the average grain size was decreased. The number of solidification nuclei in the liquid alloy that will act during solidification is inversely correlated with grain size. Since each grain originates from a single nucleus, the more nuclei there are, the more grains will form and the smaller the grain. If there are enough nuclei, globular grains of primary α-Al will preferentially develop and dendritic structures can disappear since they won't have room to expand. A fibrous silicon structure and, in certain places, a lamellar structure that is halfway between acicular and fibrous are the results of adding the Sb element to the Al-Si alloy. The addition of Sb element to the Al-Si alloy does result in a fibrous silicon structure and in some other locations in a lamellar structure that is intermediate between acicular and fibrous. Nonetheless, it has been noted that Sb can efficiently enhance the Al–Si eutectic structure, giving it superior casting qualities and a low susceptibility to gassing. Because of this, Sb has been utilized in place of Na and Sr for creating Al–Si alloys. It is commonly known that Sb refines the eutectic Si phase at concentrations of 0.05% or higher and that it functions more frequently as a eutectic silicon refining agent in Al–Si alloys. Depending on the alloy's composition, typical amounts in Sb-treated alloys reported in the literature vary from 0.05% to 0.8%. While 1.0% Sb addition resulted in the development of coarse Si particles, 0.5% Sb addition improved the microstructure of the Al-12Si alloy (Jiana. et.al, 2006).. On the other hand, when the melt is held for a long time, the Sb concentration rises from top to bottom. The disparity between the densities of Sb (~6.4 g/cm3) and Al (~2.385 g/cm3) may be the cause of this. When the melt is held at 720 °C (Brandes, 1998), antimony gradually sinks to the bottom of the crucible. According to the observations above, Sb needs some time to sink to the bottom of the melt. Additionally, a higher level of addition is observed to boost the desire to settle. According to (Prasada Rao et al. ,2008), the Sb content in Al–7Si alloy castings varies from top to bottom. Both at 0.2 and 0.5 weight percent addition, the Sb concentration drops from the top to the bottom of the casting throughout a 5-minute holding period.

Proposed mechanism of modification by Sb

AlSb is created at 657 °C as a result of the reaction between Al and Sb in the liquid as the solidification of A356 liquid proceeds from 720 °C (Prasada Rao et al., 2008). This finding implies that a higher concentration of Sb in liquid A356 does not contribute to improved eutectic silicon refining. However, some previous findings claim that constitutional super cooling is the cause of the change of eutectic silicon in Al–Si-alloys (with trace levels of Sb). Nevertheless, for a given Sb addition level, these ideas were unable to explain why eutectic silicon modified better over a longer holding period (Qiyang. et. al, 1998). Long-term storage of the Sb-treated Al–7Si alloy has been shown to cause the development of AlSb particles in the casting.

By promoting the nucleation of Si particles, these AlSb particles may improve the modification (refinement) of eutectic silicon in long-holding melts. Similar to sodium and strontium, antimony in the Al-Si eutectic melt neutralizes phosphorus. Phosphorus is dissolved by the molecule Mg_3Sb_2, which is created when antimony and magnesium interact. When magnesium is not present, antimony and aluminum combine to generate AlSb, which has an effect comparable to that of Mg_3Sb_2. In the Al-Si eutectic melt, antimony's activity is irreversible (Khan. et. al, 1994). Upon further cooling, a eutectic reaction occurs, producing Si and α-Al. These eutectic silicon needles are most likely altered by improved nucleation by liquid-soluble AlSb substrates (produced on prolonged melt holding time). Therefore, the more Sb is added, the more AlSb particles are supplied, which leads to improved modification (refinement) of the eutectic silicon particles in the fully formed A356 alloy. According to a number of researchers, the primary cause of antimony's alteration of Al-Si alloy is the development of the intermetallic phase (AlSb), which improves the refinement of the eutectic silicon particles in fully solidified form. (Uzun. et.al, 2011, Prasada Rao et.al, 2008, Bian. et.al, 2001).

.

5. CONCLUSION

This study investigates the impact of Sb element addition on the microstructure properties of A356 alloy. The study examines the microstructural changes, and also discusses the modification mechanism of the base alloy with Sb element addition. The following conclusions can be drawn:

(1) Upon inoculated by Sb element to A356, the dendritic structure of α-Al phase was broken up and converted into a somewhat globular grain structure. The average grain size was about 320 μm. The decrease in grain size could be associated with addition of Sb element. While increase addition of Sb element from 0.1% to 0.3% led to decrease in grain size from 320 to 280 μm. It can be seen that the increase of Sb element from 0 to 0.3 wt. % in the alloy can result in a fine microstructure and almost significant reduction of the average grain size.

(2) With the addition level of Sb element to A356, it can be modifiers to the A356 alloy by altered the morphology of the eutectic silicon from coarse acicular to lamellar or fibrous shape. Most of the silicon particles were transformed to rod shape with blunted tips, and rounded shape. Acicular silicon phase was completely absent and lamellar type structure turned to fully modified structure.

(3) The refinement and modification mechanism of A356 is due to the synergistic effect of Sb additions. Antimony combines with aluminium to form AlSb. On further cooling, eutectic reaction takes place, resulting in α-Al and Si. Probably, these eutectic silicon needles are modified by enhanced nucleation by AlSb substrates available in the liquid. Since each grain of α-Al forms from one single nucleus, as great the number of nuclei, as more grains will form, thus their size will reduce. If the number of nuclei is sufficiently high, dendritic structures can be avoided as they will have no space to grow, and globular grains of primary α-Al will preferentially form.

7. REFERENCES

Annual Book of ASM Standard. 2005. Metallographic, *Vol 9, pp. 620-630*

Bian X., Wang W., Qin J.,2001, Liquid Structure of Al±12.5% Si Alloy Modified by Antimony, *Materials Characterization 46, pp. 25- 29*

Brandes E.A., Brooke G.B. (Eds.). 1998, Smithells Light Metals Handbook, *Butterworth- Heinemann, OX, pp. 5-9, 117*

Hao D., Siming X., Jie L., Yu W., Lu L., and Wenbin Y., 2020. Modification of Mg_2Si Phase Morphology in Mg-4Si Alloy by Sb and Nd Additions. *Journal of Materials Engineering and Performance, p 231*

Jiana X., Meeka T.T., Hanb Q., 2006. Refinement of Eutectic Silicon Phase of Aluminium A356 alloy Using High-Intensity Ultrasonic Vibration, *Scrip Materialia 54, pp. 893–896.*

Jiana X., Xua H. , Meeka T.T., Hanb Q., 2005. Effect of Power Ultrasound on Solidification of Aluminium A356 alloy, *Materials Letters 59, pp. 190– 193.*

Karakosea E., Keskin M., 2009. Effect of Solidification Rate on the Microstructure and Micro Hardness of a Melt Spun Al–8Si–1Sb alloy. *Journal of Alloys and Compounds 479 230–236.*

Kazuhiro N., Arne K., 2001. Eutectic Growth *pp. 205-216*

KHAN S., ELLIOTT R.,1994, Effect of Antimony on the Growth of Kinetics of Aluminium-Silicon eutectic Alloys, *journal of materials science, pp. 736 – 741.*

Mode in Strontium, Antimony and Phosphorus Modified Hypoeutectic Al-Si Foundry Alloys. *Materials Tranactions, Vol. 42, No, 3 PP. 393 to 396*.

Muhammad S. U., 2Laminu S. K., and Abdulmumin A. A., 2024. Influence of Sodium Chloride Modifier on the Properties of Aluminium-Silicon Alloy *Jmme, Vol.14.*

Nataša N., Pavel K., Jan S., Tuong N. V., 2018. Influence of Ca, Sb and Heat Treatment on AlSi9CuMnNi alloy in Frame of their Properties from view of Machining. *Matec Web of Conferences 244, 02003.*

Polmear., I.J.,2006. Light Alloys from Traditional Alloys to Nanocrystals, *Fourth Edition Melbourne, Australia,*

Qiyang L. 1998, Effect of Antimony on the Growth Kinetics of High purity Al-Si Alloys, *Scripta Materialia, Vol. 38, No. 7, pp. 1083–1089*

Peng T., Jinshu L., Yixue Y., and Wanyao H., 2023. Microstructure and Mechanical Properties of Cast Al-15Mg2Si-8Si-Based alloy with Various Cr-Sb Ratio Addition, *Journal of Materials Engineering and Performance* p 773.

Prasada Rao A.K., Das K., Murty B.S., . Chakraborty M, 2008, On the Modification and Segregation Behavior of Sb in Al–7Si Alloy During Solidification, *Materials Letters 62, pp. 2013–2016.*

Puga H., Costaa S., Barbosa J., Ribeirob S., ProkicM.. 2011. Influence of Ultrasonic Melt Treatment on Microstructure and Mechanical Properties of AlSi9 Cu3 alloy, *Journal of Materials Processing Technology,*

Waly M. A. and Reif W., 1993, Thermal Analytical Son the Modification of Al- 7% Si with Addition of Sr & Na*, 6th Arab International Aluminium Conference- ARAB AL 93, Cairo, 11-14, Dec*.

Uzun O., Yılmaz F., Kolemen U., Bas N, 2011, Sb Effect on Micro Structural and Mechanical Properties of Rapidly Solidified Al–12Si alloy, *Journal of Alloys and Compounds 509, pp. 21–26.*

Yu-Chou T., Cheng-Yu C., Sheng-L. L., Chih-K. L., Jing-C L., S.W. Limc, 2009. Effect of Trace La Addition on the Microstructures and Mechanical Properties of A356 (Al–7Si–0.35Mg) aluminum alloys, Journal *of Alloys and Compounds 487, p. 157–162*

Zhu M., Yang G., Yao L., Cheng S, and Zhou Y , 2009. Influence of Al-Ti-B Addition on the Microstructure and Mechanical Properties of A356 alloys. *State Key Rare Metals Vol. 28, No. 2, Apr 2009, p. 181*

Zhongtao Z., Jie L., Hongyun Y., Jian Z., Tingju L., 2009. Microstructure Evolution of A356 Alloy Under Compound Field, *Journal of Alloys and Compounds 484, pp. 458–462.*